



ELSEVIER

Available online at www.sciencedirect.com

SCIENCE @ DIRECT®

Comput. Methods Appl. Mech. Engrg. 195 (2006) 2313–2333

**Computer methods
in applied
mechanics and
engineering**

www.elsevier.com/locate/cma

Objective energy–momentum conserving integration for the constrained dynamics of geometrically exact beams

S. Leyendecker^a, P. Betsch^b, P. Steinmann^{a,*}

^a *Chair of Applied Mechanics, Department of Mechanical Engineering, P.O. Box 3049, University of Kaiserslautern, 67653 Kaiserslautern, Germany*

^b *Chair of Computational Mechanics, Department of Mechanical Engineering, University of Siegen, Paul-Bonatz-Straße 9-11, 57068 Siegen, Germany*

Received 26 April 2005; accepted 9 May 2005

Abstract

In this paper the results in [S. Leyendecker, P. Betsch, P. Steinmann, Energy-conserving integration of constrained Hamiltonian systems—a comparison of approaches, *Comput. Mech.* 33 (2004) 174–185] are extended to geometrically exact beams. The finite element formulation for nonlinear beams in terms of directors, providing a framework for the objective description of their dynamics, is considered. Geometrically exact beams are analysed as Hamiltonian systems subject to holonomic constraints with a Hamiltonian being invariant under the action of $SO(3)$. The reparametrisation of the Hamiltonian in terms of the invariants of $SO(3)$ is perfectly suited for a temporal discretisation which leads to energy–momentum conserving integration. In this connection the influence of alternative procedures, the Lagrange multiplier method, the Penalty method and the augmented Lagrange method, for the treatment of the constraints is investigated for the example of a beam with concentrated masses.

© 2005 Elsevier B.V. All rights reserved.

Keywords: Geometrically exact beams; Constrained Hamiltonian systems; Energy–momentum schemes

1. Introduction

Modelling geometrically exact beams as a special Cosserat continuum (see e.g. [2]) has been the basis for many finite element formulations starting with the work of Simo [3]. The formulation of the beam dynamics

* Corresponding author. Tel.: +49 0 631 205 2419; fax: +49 0 631 205 2128.

E-mail addresses: slauer@rhrk.uni-kl.de (S. Leyendecker), betsch@imr.mb.uni-siegen.de (P. Betsch), ps@rhrk.uni-kl.de (P. Steinmann).

as Hamiltonian system subject to internal constraints, which are associated with the kinematic assumptions of the underlying continuous theory, has several advantages. It allows the incorporation of constraints on configuration level as well as on momentum level in a systematic way. The spatial interpolation of the director triad, which is constrained to be orthonormal in each node of the central line of the beam, leads to objective strain measures in the spatially discretised configuration. This idea is developed independently in [4,5].

While the authors in [5] restrict themselves to the specification of the weak form of balance equations for the beam in the static case, in [6] the equations of motion are given as Hamiltonian system subject to holonomic constraints, which are realised with the Lagrange multiplier method. The Hamiltonian formalism provides the possibility to use different methods for the constraint enforcement. In [1] the Lagrange multiplier method, the Penalty method and the augmented Lagrange method for the treatment of holonomic constraints are compared and the results are illustrated with the examples of mass point systems. The same methods are used here for the realisation of the internal constraints of the beam.

In this work the semi-discrete Hamiltonian system for the beam in [6] is modified in two ways leading to the following beneficial aspects. First of all the enforcement of the constraints is described more generally, independent of the used method, thus different methods can be inserted into the formulation. Secondly the Hamiltonian is reparametrised. Since objectivity of the strain measures is a main goal of the formulation, it suggests itself to parametrise the rotationally invariant Hamiltonian directly in the invariants of the Lie group $SO(3)$. Consequently the strain measures are approximated objectively. This is an ideal basis for a temporal discretisation using the concept of G -equivariant discrete derivatives by Gonzalez [7], which leads to energy–momentum conserving time-integration of the equations of motion. Thus a time-stepping scheme is obtained, which is objective and by construction energy–momentum preserving.

Section 2 addresses the general description of mechanical systems as constrained Hamiltonian systems, whereby the mentioned methods to treat the constraints and the correlation between the solutions of the corresponding discrete systems are mentioned. In Section 3 the modelling of geometrically exact beams as a special Cosserat continuum is presented shortly and the constrained Hamiltonian equations of motion are formulated. Their spatial discretisation by isoparametric finite elements is presented in Section 3.3, leading to objective strain measures in the semi-discrete configuration. After the reparametrisation of the isotropic Hamiltonian and a brief description of the concept of G -equivariant discrete derivatives in Section 3.4, the fully discrete equations for the beam dynamics are given using different methods for the constraint enforcement. These are solved for the example of a beam with concentrated masses and the results, especially the constraint fulfilment, are compared in Section 4.

2. Hamiltonian systems subject to holonomic constraints

The dynamics of mechanical systems is described as Hamiltonian system subject to holonomic constraints. Hereby the Hamiltonian is a \mathcal{C}^1 -function $H : \mathcal{P} \rightarrow \mathbb{R}$ and $\mathcal{P} = T^*\mathcal{Q}$ is a $2n$ -dimensional linear phase space with the canonical (time-dependent) coordinates

$$\mathbf{z}(t) = [\mathbf{q}(t), \mathbf{p}(t)] = [q^1(t), \dots, q^n(t), p_1(t), \dots, p_n(t)], \quad t \in \mathcal{T}, \quad n \in \mathbb{N}.$$

$\mathcal{T} \subset \mathbb{R}$ denotes a bounded interval of the time-axis. We suppose that only scleronomic and holonomic constraints, possibly together with their temporally differentiated form, are present. Furthermore all appearing external loads are assumed to be conservative, such that the Hamiltonian represents the total energy of the system. For a problem of nonlinear elasticity, the total energy consists of the sum of kinetic

energy $T : \mathcal{P} \rightarrow \mathbb{R}$ and potential energy $V : \mathcal{P} \rightarrow \mathbb{R}$ that can be decomposed additively into V_{ext} , taking into account conservative external loads, and V_{int} , accounting for elastic deformations. Then in terms of the Hamiltonian vector field X_H and the symplectic matrix \mathbb{J} , Hamilton’s equations take the form

$$\dot{\mathbf{z}}(t) = X_H(\mathbf{z}(t)) = \mathbb{J} \cdot \nabla H. \tag{1}$$

Let the motion of the mechanical system be constrained by m_1 holonomic, scleronomic configuration constraints $\tilde{g}_1(\mathbf{q}) = \dots = \tilde{g}_{m_1}(\mathbf{q}) = 0$. Since in the Hamiltonian formalism, the configuration variable $\mathbf{q}(t)$ and the corresponding conjugate momentum $\mathbf{p}(t)$ are dealt with on an equal footing, the consistency condition, that the configuration constraints must be satisfied for all times, must hold. This leads to the temporally differentiated form of the constraints $d\tilde{g}_i/dt = \nabla \tilde{g}_i(\mathbf{q}) \cdot \dot{\mathbf{q}} = \nabla \tilde{g}_i(\mathbf{q}) \cdot D_p H = 0$, $i = 1, \dots, m_1$, where (1) has been taken into account. For a concise representation \tilde{g}_i and $d\tilde{g}_i/dt$ are combined to

$$\begin{bmatrix} g_1(\mathbf{z}) \\ \vdots \\ g_m(\mathbf{z}) \end{bmatrix} = \mathbf{g}(\mathbf{z}) = \mathbf{0} \quad \text{with } g_i : \mathcal{P} \rightarrow \mathbb{R} \text{ smooth, } \quad i = 1, \dots, m = 2m_1 \tag{2}$$

and it is assumed that $\mathbf{0}$ is a regular value of the constraints (see e.g. [8,9]).

The treatment of the constraints shall be represented generally by the scalar valued \mathcal{C}^1 -function $\tilde{P} : \mathbf{g}(\mathcal{P}) \rightarrow \mathbb{R}$ that is required to be of the form

$$\tilde{P}(\mathbf{g}(\mathbf{z})) \geq 0 \quad \forall \mathbf{z} \quad \text{and} \quad \tilde{P}(\mathbf{g}(\mathbf{z})) = 0 \iff \mathbf{g}(\mathbf{z}) = \mathbf{0}. \tag{3}$$

In order to unify the domains of the functions composing H , we introduce $P : \mathcal{P} \rightarrow \mathbb{R}$ with $P(\mathbf{z}) = \tilde{P}(\mathbf{g}(\mathbf{z}))$.

A deviation of the mechanical system from the constraint manifold $\mathcal{C} = \mathbf{g}^{-1}(\mathbf{0}) \subset \mathcal{P}$ is interpreted as a contribution to the systems total energy, thus for constrained Hamiltonian systems P is added to the energies $T + V$, such that the now relevant augmented Hamiltonian $H : \mathcal{P} \rightarrow \mathbb{R}$ reads

$$H(\mathbf{z}) = T(\mathbf{z}) + V(\mathbf{z}) + P(\mathbf{z}). \tag{4}$$

According to the method used to treat the constraints, the additional function P takes different forms. In [1], special forms of P and the Hamiltonian systems (1) emanating from (4) are described in detail for the Lagrange multiplier method, the Penalty method and the augmented Lagrange method. The known equivalences between the solutions of the different continuous systems (see e.g. [10,11]) are carried over to the corresponding discrete systems, that have been temporally discretised using the discrete derivative by Gonzalez [7]. The equivalence of the discrete Penalty system (in the limit for penalty parameters tending to infinity) and of the discrete Augmented Lagrange system (in the limit for infinitely many Augmented Lagrange iterations) to the discrete Lagrange Multiplier system is proved there. In this work, these theoretical results are extended to the nonlinear elastic beam theory.

3. Objective formulation of the geometrically exact beam as constrained Hamiltonian system

3.1. Kinematics

In [5] Betsch and Steinmann introduce frame-indifferent finite elements for the geometrically exact beam theory, in the sense that they inherit the objectivity of the underlying continuous beam strains. The concept

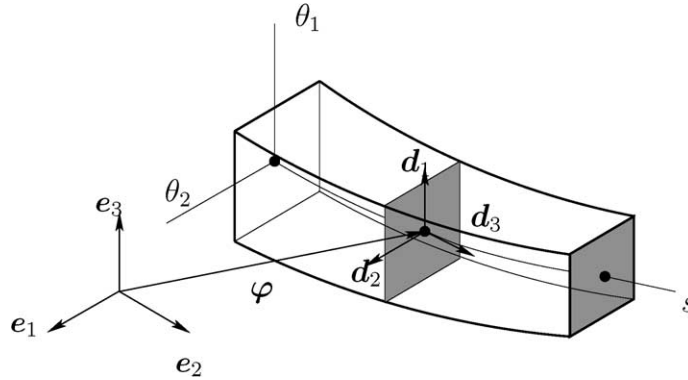


Fig. 1. Configuration of a beam.

relies on the kinematic assumption illustrated in Fig. 1 (cf. [2]) that the placement of a material point, identified by its position vector $\mathbf{X}(\theta^i) \in \mathbb{R}^3$ in the reference configuration \mathcal{B}_0 , can be described by

$$\mathbf{x}(\theta^\alpha, s, t) = \boldsymbol{\varphi}(s, t) + \theta^\alpha \mathbf{d}_\alpha(s, t). \tag{5}$$

Einstein summation convention is used to sum over repeated indices, Greek indices take the values 1 and 2, whereas Latin indices range from 1 to 3. $(\theta^1, \theta^2, \theta^3 = s) \in \mathbb{R}^3$ is a triple of curvilinear coordinates with $s \in [0, L] \subset \mathbb{R}$ being the arc-length of the line of centroids $\boldsymbol{\varphi}(s, 0) \in \mathbb{R}^3$. The director triad $\mathbf{d}_i(s, t) \in \mathbb{R}^3$, $i = 1, 2, 3$ is assumed to be orthonormal, and $\mathbf{d}_1(s, t)$, $\mathbf{d}_2(s, t)$ characterise the configuration of the cross-section at s and time t .

This work is built on the formulation of the dynamics of geometrically exact beams in [6]. Therefore this formulation is presented in short.

Remark 1. Setting up the Lagrangian $L : T\mathcal{Q} \rightarrow \mathbb{R}$, $L = L(\mathbf{x}, \dot{\mathbf{x}})$ where \mathbf{x} is specified in (5) and $\dot{\mathbf{x}}$ denotes its temporal derivative, one comes across the fact, that the kinetic energy is independent of $\dot{\mathbf{d}}_3$. Due to that property, the Lagrangian is degenerate and it follows that $\mathbf{p}_3 = \frac{\partial L}{\partial \dot{\mathbf{d}}_3} = \mathbf{0}$. One can still pass to the Hamiltonian formulation using Dirac's theory (see [6,12] and references therein). Thereby the relevant momenta are $\bar{\mathbf{p}} = (\mathbf{p}_\varphi, \mathbf{p}_1, \mathbf{p}_2)$. Setting $\bar{\mathbf{q}} = (\boldsymbol{\varphi}, \mathbf{d}_1, \mathbf{d}_2)$, the Hamiltonian depends on the (reduced) phase space variable $\mathbf{z} = \mathbf{z}(s, t)$ with

$$\mathbf{z} = [\bar{\mathbf{q}}, \bar{\mathbf{p}}] = [\bar{\mathbf{q}}, \mathbf{d}_3, \bar{\mathbf{p}}] = [\boldsymbol{\varphi}, \mathbf{d}_1, \mathbf{d}_2, \mathbf{d}_3, \mathbf{p}_\varphi, \mathbf{p}_1, \mathbf{p}_2] \in \mathbb{R}^{21}. \tag{6}$$

3.2. Dynamics of the beam as Hamiltonian system subject to internal constraints

The beams kinetic energy can be written in the form

$$T(\mathbf{z}(t)) = \frac{1}{2} \int_0^L \bar{\mathbf{p}} \cdot \bar{\mathbf{M}} \cdot \bar{\mathbf{p}} \, ds, \tag{7}$$

with the nonsingular reduced mass matrix (see Remark 1)

$$\bar{\mathbf{M}} = \begin{bmatrix} A_\rho \mathbf{I} & \mathbf{0} & \mathbf{0} \\ \mathbf{0} & M_\rho^1 \mathbf{I} & \mathbf{0} \\ \mathbf{0} & \mathbf{0} & M_\rho^2 \mathbf{I} \end{bmatrix}, \tag{8}$$

where \mathbf{I} and $\mathbf{0}$ denote the 3×3 identity and zero matrices respectively, A_ρ is the mass density per reference length and M_ρ^1, M_ρ^2 can be interpreted as principal mass-moments of inertia of the cross-section.

In the present case, the potential energy function is assumed to be the sum of stored and external energy

$$V(\mathbf{z}(t)) = V_{\text{int}}(\mathbf{z}(t)) + V_{\text{ext}}(\mathbf{z}(t)) = \int_0^L W_{\text{int}}(\boldsymbol{\Gamma}(\mathbf{q}), \mathbf{K}(\mathbf{q})) \, ds + \int_0^L W_{\text{ext}}(\mathbf{q}) \, ds. \tag{9}$$

W_{int} is a strain energy density function expressed in terms of the objective strain measures

$$\begin{aligned} \boldsymbol{\Gamma}(\mathbf{q}) &= \Gamma_i \mathbf{e}_i \quad \text{and} \quad \Gamma_i = \mathbf{d}_i \cdot \boldsymbol{\varphi}_{,s} - \delta_{i3}, \\ \mathbf{K}(\mathbf{q}) &= K_i \mathbf{e}_i \quad \text{and} \quad K_i = \frac{1}{2} \epsilon_{ijk} [\mathbf{d}_k \cdot \mathbf{d}_{j,s} - [\mathbf{d}_k \cdot \mathbf{d}_{j,s}]|_{t=0}], \end{aligned} \tag{10}$$

where δ_{ij} is the Kronecker delta, ϵ_{ijk} is the alternating symbol and $\{\mathbf{e}_i\}$ an orthonormal basis which is fixed in space. An interpretation of these strain measures can be found in [2], whereupon Γ_1 and Γ_2 measure shear strains, Γ_3 elongation, K_1 and K_2 quantify flexure and K_3 torsion. W_{ext} is the density of the conservative external loads.

The assumption of orthonormality of the director triad gives rise to $m_1 = 6$ independent holonomic internal constraints at each point of the central line of the beam

$$\mathbf{g}(\mathbf{z}) = \begin{bmatrix} \frac{1}{2}[\mathbf{d}_1 \cdot \mathbf{d}_1 - 1] \\ \frac{1}{2}[\mathbf{d}_2 \cdot \mathbf{d}_2 - 1] \\ \frac{1}{2}[\mathbf{d}_3 \cdot \mathbf{d}_3 - 1] \\ \mathbf{d}_1 \cdot \mathbf{d}_2 \\ \mathbf{d}_1 \cdot \mathbf{d}_3 \\ \mathbf{d}_2 \cdot \mathbf{d}_3 \end{bmatrix}. \tag{11}$$

Remark 2. The investigation of several numerical examples of geometrically exact beams (e.g. in [5,6]) has brought forward that the incorporation of the temporally differentiated form of the constraints on momentum level (so called secondary constraints, see [12,13]) has not lead to crucial advantages (besides the fulfilment of the secondary constraints themselves). The solution of the Hamiltonian system has not been influenced considerably by their fulfilment. Therefore in the sequel we restrict ourselves to the enforcement of the constraints on configuration level, although the Hamiltonian formalism would allow for the incorporation of secondary constraints in an obvious systematic way.

The extra function P to treat the constraints is assumed to be composed of the functions $\mathbf{v} = \mathbf{v}(s, t)$, $\mathbf{R} = \mathbf{R}(\mathbf{g}(\mathbf{z}(s, t)))$ with $(s, t) \in [0, L] \times \mathcal{T}$. The product of \mathbf{v} and \mathbf{R} must be scalar, but their range is not specified. Further conditions on \mathbf{v} , \mathbf{R} can be deduced from (3). Then the contribution of the (unfulfilled) constraints to the energy of the beam can be calculated as

$$P(\mathbf{z}(t)) = \int_0^L \mathbf{v}(s, t) \mathbf{R}(\mathbf{g}(\mathbf{z}(s, t))) \, ds. \tag{12}$$

As mentioned in Remark 1 Dirac’s theory must be used to derive the equations of motion for the geometrically exact beam in the Hamiltonian formalism. The transition from the Lagrangian formulation (with a degenerate Lagrangian) to the Hamiltonian formulation is performed in detail in [6]. Along the lines described there and neglecting the secondary constraints (see Remark 2) and treating the primary constraints generally by the function in (12), we arrive at the following equations of motion for the geometrically exact beam, which have to be solved for $\mathbf{z} = [\mathbf{q}, \bar{\mathbf{p}}] = [\bar{\mathbf{q}}, \mathbf{d}_3, \bar{\mathbf{p}}]$:

$$\begin{aligned}
 \dot{\bar{\mathbf{q}}}(s, t) &= \delta_{\bar{\mathbf{p}}} T(\mathbf{z}(s, t)), \\
 \dot{\bar{\mathbf{p}}}(s, t) &= -\delta_{\bar{\mathbf{q}}} V(\mathbf{z}(s, t)) - \delta_{\bar{\mathbf{q}}} P(\mathbf{z}(s, t)), \\
 \mathbf{0} &= -\delta_{\mathbf{d}_3} V(\mathbf{z}(s, t)) - \delta_{\mathbf{d}_3} P(\mathbf{z}(s, t)).
 \end{aligned}
 \tag{13}$$

Remark 3. If the Lagrange multiplier method is used to enforce the constraints, the system (13) is supplemented by the constraint equation (11) resulting in an system of DAEs.

3.3. Hamiltonian formulation of the semi-discrete beam

To perform a discretisation in space, n_{node} nodes subdivide the central line of the beam into finite elements. We introduce isoparametric finite element interpolations using Lagrange-type nodal shape functions $N_A(s)$ and Dirac deltas $M_A(s) = \delta(s - s_A)$ associated with the nodal points $s_A \in [0, L]$, $A = 1, \dots, n_{\text{node}}$

$$\begin{aligned}
 \boldsymbol{\varphi}^h(s, t) &= \sum_{A=1}^{n_{\text{node}}} N_A(s) \boldsymbol{\varphi}^A(t), & \mathbf{d}_k^h(s, t) &= \sum_{A=1}^{n_{\text{node}}} N_A(s) \mathbf{d}_k^A(t), \quad k = 1, 2, 3, \\
 \mathbf{p}_\varphi^h(s, t) &= \sum_{A=1}^{n_{\text{node}}} N_A(s) \mathbf{p}_\varphi^A(t), & \mathbf{p}_k^h(s, t) &= \sum_{A=1}^{n_{\text{node}}} N_A(s) \mathbf{p}_k^A(t), \quad k = 1, 2, \\
 \mathbf{z}^h(s, t) &= \sum_{A=1}^{n_{\text{node}}} N_A(s) \mathbf{z}^A(t), & \mathbf{v}^h(s, t) &= \sum_{A=1}^{n_{\text{node}}} M_A(s) \mathbf{v}^A(t).
 \end{aligned}
 \tag{14}$$

Thus the semi-discrete mechanical system is characterised by the phase vector

$$\begin{aligned}
 \mathbf{z}(t) &= [\mathbf{z}^1(t), \dots, \mathbf{z}^{n_{\text{node}}}(t)] \in \mathbb{R}^{21n_{\text{node}}} & \text{with } \mathbf{z}^A(t) &= [\mathbf{q}^A(t), \bar{\mathbf{p}}^A(t)] \in \mathbb{R}^{21}, \\
 \mathbf{q}(t) &= [\mathbf{q}^1(t), \dots, \mathbf{q}^{n_{\text{node}}}(t)] \in \mathbb{R}^{12n_{\text{node}}} & \text{with } \mathbf{q}^A(t) &= [\boldsymbol{\varphi}^A, \mathbf{d}_1^A, \mathbf{d}_2^A, \mathbf{d}_3^A](t) \in \mathbb{R}^{12}, \\
 \bar{\mathbf{p}}(t) &= [\bar{\mathbf{p}}^1(t), \dots, \bar{\mathbf{p}}^{n_{\text{node}}}(t)] \in \mathbb{R}^{9n_{\text{node}}} & \text{with } \bar{\mathbf{p}}^A(t) &= [\mathbf{p}_\varphi^A, \mathbf{p}_1^A, \mathbf{p}_2^A](t) \in \mathbb{R}^9.
 \end{aligned}
 \tag{15}$$

Insertion of (14) and (15) into the kinetic energy (7) yields

$$T^h(\mathbf{z}(t)) = \frac{1}{2} \sum_{A,B=1}^{n_{\text{node}}} \bar{\mathbf{p}}^A(t) \cdot (\bar{\mathbf{M}}_{AB}^h)^{-1} \cdot \bar{\mathbf{p}}^B(t) = \frac{1}{2} \bar{\mathbf{p}}(t) \cdot (\bar{\mathbf{M}}^h)^{-1} \cdot \bar{\mathbf{p}}(t),
 \tag{16}$$

with the consistent mass matrix

$$\begin{aligned}
 \bar{\mathbf{M}}_{AB}^h &= \begin{bmatrix} M_{AB} \mathbf{I} & \mathbf{0} & \mathbf{0} \\ \mathbf{0} & M_{AB}^1 \mathbf{I} & \mathbf{0} \\ \mathbf{0} & \mathbf{0} & M_{AB}^2 \mathbf{I} \end{bmatrix}, \\
 M_{AB} &= \int_0^L A_\rho N_A(s) N_B(s) \, ds, & M_{AB}^z &= \int_0^L M_\rho^z N_A(s) N_B(s) \, ds.
 \end{aligned}
 \tag{17}$$

Remark 4. Provided that the nodes are numbered appropriately, for a k -node beam element, the compact support of the shape functions N_A , $A = 1, \dots, k$ causes $M_{AB} = M_{AB}^1 = M_{AB}^2 = 0$ for $|A - B| \geq k$. Thus the symmetric, global mass matrix $\bar{\mathbf{M}}^h$ is banded with nonzero elements on the diagonal and on $k - 1$ subdiagonals.

Insertion of $\mathbf{v}^h(s, t)$ in (14) into (12) yields

$$P^h(\mathbf{z}(t)) = \sum_{A=1}^{n_{\text{node}}} \mathbf{v}^A(t) \mathbf{R}(\mathbf{g}(\mathbf{z}^A(t))), \tag{18}$$

i.e. the constraint fulfilment is enforced at the nodes.

After the spatial discretisation (14) and (15) has been inserted, the potential energy (9) reads

$$V^h(\mathbf{z}(t)) = \int_0^L W_{\text{int}}(\mathbf{\Gamma}(\mathbf{q}^h(s, t)), \mathbf{K}(\mathbf{q}^h(s, t))) \, ds + \int_0^L W_{\text{ext}}(\mathbf{q}^h(s, t)) \, ds. \tag{19}$$

The special form of (19) depends on the behaviour of the material under consideration and on the external potential.

Example 5. Let the external conservative load be the gravitation with gravitational constant g and define $\mathbf{g}^T = [0, 0, g, 0, 0, 0, 0, 0]$.

$$\begin{aligned} V_{\text{ext}}^h(\mathbf{z}(t)) &= \int_0^L W_{\text{ext}}(\mathbf{q}^h(s, t)) \, ds = \int_0^L \mathbf{g} \cdot \overline{\mathbf{M}} \cdot \overline{\mathbf{q}}^h(s, t) \, ds \\ &= \sum_{A=1}^{n_{\text{node}}} \mathbf{g} \cdot \overline{\mathbf{M}} \cdot \overline{\mathbf{q}}^A(t) \int_0^L N_A(s) \, ds = \sum_{A=1}^{n_{\text{node}}} W_{\text{ext}}^A(\mathbf{q}^A(t)). \end{aligned} \tag{20}$$

Example 6. Assume that the hyperelastic material behaviour of the beam is governed by the stored-energy function

$$W_{\text{int}}(\mathbf{\Gamma}, \mathbf{K}) = \frac{1}{2} \mathbf{\Gamma} \cdot \mathbf{D}^{\Gamma} \cdot \mathbf{\Gamma} + \frac{1}{2} \mathbf{K} \cdot \mathbf{D}^{\mathbf{K}} \cdot \mathbf{K}, \tag{21}$$

with

$$\mathbf{D}^{\Gamma} = \begin{bmatrix} GA_1 & 0 & 0 \\ 0 & GA_2 & 0 \\ 0 & 0 & EA \end{bmatrix}, \quad \mathbf{D}^{\mathbf{K}} = \begin{bmatrix} EI_1 & 0 & 0 \\ 0 & EI_2 & 0 \\ 0 & 0 & GJ \end{bmatrix}. \tag{22}$$

Insertion into (19) yields

$$\begin{aligned} V_{\text{int}}^h(\mathbf{z}(t)) &= \frac{1}{2} \sum_{i=1}^3 D_{ii}^{\Gamma} \underbrace{\int_0^L (\Gamma_i(\mathbf{q}^h(s, t)))^2 \, ds}_{\doteq} + D_{ii}^{\mathbf{K}} \underbrace{\int_0^L (K_i(\mathbf{q}^h(s, t)))^2 \, ds}_{\doteq} \\ &= \frac{1}{2} \sum_{i=1}^3 D_{ii}^{\Gamma} \Gamma_i^h(\mathbf{q}(t)) + D_{ii}^{\mathbf{K}} K_i^h(\mathbf{q}(t)) = \sum_{i=1}^3 W_{\text{int}}^i(\mathbf{\Gamma}^h(\mathbf{q}(t)), \mathbf{K}^h(\mathbf{q}(t))), \end{aligned} \tag{23}$$

where

$$W_{\text{int}}^i(\mathbf{\Gamma}^h(\mathbf{q}(t)), \mathbf{K}^h(\mathbf{q}(t))) = \frac{1}{2} [D_{ii}^{\Gamma} \Gamma_i^h(\mathbf{q}(t)) + D_{ii}^{\mathbf{K}} K_i^h(\mathbf{q}(t))], \quad i = 1, 2, 3. \tag{24}$$

The composition of (16), (18) and (19) yields the Hamiltonian for the semi-discrete beam $H^h(\mathbf{z}(t)) = T^h(\mathbf{z}(t)) + V^h(\mathbf{z}(t)) + P^h(\mathbf{z}(t))$ and the semi-discrete Hamiltonian system of equations, which has to be solved for $\mathbf{z}^A(t)$, $A = 1, \dots, n_{\text{node}}$

$$\begin{aligned}
 \dot{\mathbf{q}}^A(t) &= D_{\bar{\mathbf{p}}^A} T^h(\mathbf{z}(t)), \\
 \dot{\bar{\mathbf{p}}}^A(t) &= -D_{\bar{\mathbf{q}}^A} V^h(\mathbf{z}(t)) - D_{\bar{\mathbf{q}}^A} P^h(\mathbf{z}(t)), \\
 \mathbf{0} &= -D_{\mathbf{d}_3^A} V^h(\mathbf{z}(t)) - D_{\mathbf{d}_3^A} P^h(\mathbf{z}(t)).
 \end{aligned}
 \tag{25}$$

3.3.1. Objectivity of the discrete strain measures

Insertion of the interpolation (14) for \mathbf{q}^h in (10) yields the discrete strain measures $\Gamma(\mathbf{q}^h)$, $\mathbf{K}(\mathbf{q}^h)$, which inherit the objectivity of the underlying geometrically exact beam theory. Consider rigid body motions of the discrete beam configuration

$$(\boldsymbol{\varphi}^A)^\sharp = \mathbf{c} + \mathbf{Q} \cdot \boldsymbol{\varphi}^A, \quad (\mathbf{d}_k^A)^\sharp = \mathbf{Q} \cdot \mathbf{d}_k^A,
 \tag{26}$$

with $\mathbf{c}(t) \in \mathbb{R}^3$ and $\mathbf{Q}(t) \in SO(3)$. Then for all $s \in [0, L]$ and $i = 1, 2, 3$ the following statements hold:

$$\Gamma_i((\mathbf{q}^h)^\sharp) = \Gamma_i(\mathbf{q}^h), \quad K_i((\mathbf{q}^h)^\sharp) = K_i(\mathbf{q}^h).
 \tag{27}$$

The proof and further details can be found in [5].

3.4. Objective energy–momentum conserving time-stepping scheme

The objectivity of the strain measures relies on the fact that $\Gamma_i, K_i, i = 1, 2, 3$ are scalar-valued isotropic functions of the vector argument \mathbf{q} . Thus they do not depend on the full vector \mathbf{q} , but on the scalar products of the vectors $\{\boldsymbol{\varphi}^J, \mathbf{d}_1^J, \mathbf{d}_2^J, \mathbf{d}_3^J, \boldsymbol{\varphi}^J, \mathbf{d}_1^J, \mathbf{d}_2^J, \mathbf{d}_3^J | J = 1, \dots, n_{\text{node}}\}$, which are invariant with respect to superposed rigid body motion. Consequently, V_{int} is an isotropic function. Detailed inspection of the kinetic energy of the discrete beam (16) and the extra function to enforce the constraints (18) shows that these parts of the Hamiltonian are rotationally invariant as well.

Remark 7. From (20) we see that in Example 5 V_{ext}^h is invariant under rotations about the gravitational axis only, whereas T^h, P^h and V_{int}^h are invariant under the action of the full Lie group $SO(3)$. From now on we assume that V_{ext}^h is invariant under the action of all elements of $SO(3)$ as well, thus the composition $H^h(\mathbf{z}(t)) = T^h(\mathbf{z}(t)) + V^h(\mathbf{z}(t)) + P^h(\mathbf{z}(t))$ is also invariant under the action of $SO(3)$. Therewith we exclude Example 5 in our theoretical considerations.

These considerations suggests to parametrise the entire isotropic Hamiltonian in the invariants of the Lie group $SO(3)$.

3.4.1. Invariance of the Hamiltonian under the action of $SO(3)$

Assume that the semi-discrete Hamiltonian H^h is invariant under the action of the Lie group $SO(3)$, i.e.

$$\begin{aligned}
 H^h(\mathbf{z}) &= H^h(\mathbf{Q} \circ \mathbf{z}) \quad \forall \mathbf{Q} \in SO(3), \quad \forall \mathbf{z} \in \mathcal{P} = \mathbb{R}^{21n_{\text{node}}} \\
 \text{with } \mathbf{Q} \circ \mathbf{z} &= (\mathbf{Q} \cdot \boldsymbol{\varphi}, \mathbf{Q} \cdot \mathbf{d}_1, \mathbf{Q} \cdot \mathbf{d}_2, \mathbf{Q} \cdot \mathbf{d}_3, \mathbf{Q} \cdot \mathbf{p}_\varphi, \mathbf{Q} \cdot \mathbf{p}_1, \mathbf{Q} \cdot \mathbf{p}_2).
 \end{aligned}
 \tag{28}$$

Then H^h is an isotropic, scalar valued function with vector arguments, hence by Cauchys Representation Theorem (cf. [2]) H^h can be expressed in terms of the invariants

$$S(\mathbf{z}^1, \dots, \mathbf{z}^{n_{\text{node}}}) = \left\{ \mathbf{y}^A \cdot \mathbf{y}^B \mid 1 \leq A \leq B \leq n_{\text{node}}, \mathbf{y}^J \in \{\boldsymbol{\varphi}^J, \mathbf{d}_1^J, \mathbf{d}_2^J, \mathbf{d}_3^J, \mathbf{p}_\varphi^J, \mathbf{p}_1^J, \mathbf{p}_2^J\} \right\}.
 \tag{29}$$

S is the set of all possible scalar products of the three-dimensional vectors composing the phase vector \mathbf{z} in (15) and contains $\frac{1}{2}[7n_{\text{node}} + 1]7n_{\text{node}}$ elements.

Remark 8. The elements of S are functionally dependent in the sense of Olver [14]. The Lie group $SO(3)$ operates semi-regularly on the $k = 21n_{\text{node}}$ -dimensional phase space \mathcal{P} with orbits of dimension $s = 3$.

According to Theorem 2.17 in [14] there exist precisely $d = k - s = 21n_{\text{node}} - 3$ independent invariants $\pi_i : \mathcal{P} \rightarrow \mathbb{R}$ composing the maximal set $\mathbf{\Pi} = [\pi_1, \dots, \pi_d]^T$. The invariants $\pi_1(\mathbf{z}), \dots, \pi_d(\mathbf{z})$ are functionally independent if and only if the Jacobian $D\mathbf{\Pi}(\mathbf{z}) \in \mathbb{R}^{d \times 21n_{\text{node}}}$ is of rank d for each $\mathbf{z} \in \mathcal{P}$. Any other invariant $\pi_e, e > d$ of the group action does depend on the quotient space $\mathcal{P}/SO(3) \cong \mathbf{\Pi}(\mathcal{P})$, i.e. it is of the form $\pi_e(\mathbf{z}) = \pi_e(\pi_1(\mathbf{z}), \dots, \pi_d(\mathbf{z}))$.

If a maximal set $\mathbf{\Pi}$ of independent invariants can be found, then the Hamiltonian can be reduced to

$$\widehat{H}^h : \mathbf{\Pi}(\mathcal{P}) \rightarrow \mathbb{R} \quad \text{with} \quad \widehat{H}^h(\mathbf{\Pi}(\mathbf{z})) = H^h(\mathbf{z}). \tag{30}$$

The invariance of the Hamiltonian under the action of a Lie group G (so called G -invariance) leads to the temporal conservation of a momentum map $J : \mathcal{P} \rightarrow T_e^*G$ along the solution of the Hamiltonian system (25) in the sense that the momentum map $\sum_{A=1}^{n_{\text{node}}} J(\mathbf{z}^A(t)) = \text{const}$ for all $t \in \mathcal{T}$. For $G = SO(3)$, the momentum map is the sum of the angular momentum at each node $J(\mathbf{z}^A) = \mathbf{q}^A \times \mathbf{p}^A$.

The set of invariants S comprises the elements

$$\begin{aligned} \pi_1^{AB}(\mathbf{z}) &= \boldsymbol{\varphi}^A \cdot \boldsymbol{\varphi}^B, & \pi_2^{AB}(\mathbf{z}) &= \mathbf{d}_1^A \cdot \mathbf{d}_1^B, & \pi_3^{AB}(\mathbf{z}) &= \mathbf{d}_2^A \cdot \mathbf{d}_2^B, & \pi_4^{AB}(\mathbf{z}) &= \mathbf{d}_3^A \cdot \mathbf{d}_3^B, \\ \pi_5^{AB}(\mathbf{z}) &= \mathbf{p}_\varphi^A \cdot \mathbf{p}_\varphi^B, & \pi_6^{AB}(\mathbf{z}) &= \mathbf{p}_1^A \cdot \mathbf{p}_1^B, & \pi_7^{AB}(\mathbf{z}) &= \mathbf{p}_2^A \cdot \mathbf{p}_2^B, & \pi_8^{AB}(\mathbf{z}) &= \boldsymbol{\varphi}^A \cdot \mathbf{d}_1^B, \\ \pi_9^{AB}(\mathbf{z}) &= \boldsymbol{\varphi}^A \cdot \mathbf{d}_2^B, & \pi_{10}^{AB}(\mathbf{z}) &= \boldsymbol{\varphi}^A \cdot \mathbf{d}_3^B, & \pi_{11}^{AB}(\mathbf{z}) &= \mathbf{d}_1^A \cdot \mathbf{d}_2^B, & \pi_{12}^{AB}(\mathbf{z}) &= \mathbf{d}_3^A \cdot \mathbf{d}_1^B, \\ \pi_{13}^{AB}(\mathbf{z}) &= \mathbf{d}_2^A \cdot \mathbf{d}_3^B, & \pi_{14}^{AB}(\mathbf{z}) &= \mathbf{p}_\varphi^A \cdot \mathbf{p}_1^B, & \pi_{15}^{AB}(\mathbf{z}) &= \mathbf{p}_\varphi^A \cdot \mathbf{p}_2^B, & \pi_{16}^{AB}(\mathbf{z}) &= \mathbf{p}_1^A \cdot \mathbf{p}_2^B, \\ \pi_{17}^{AB}(\mathbf{z}) &= \boldsymbol{\varphi}^A \cdot \mathbf{p}_\varphi^B, & \pi_{18}^{AB}(\mathbf{z}) &= \boldsymbol{\varphi}^A \cdot \mathbf{p}_1^B, & \pi_{19}^{AB}(\mathbf{z}) &= \boldsymbol{\varphi}^A \cdot \mathbf{p}_2^B, & \pi_{20}^{AB}(\mathbf{z}) &= \mathbf{d}_1^A \cdot \mathbf{p}_\varphi^B, \\ \pi_{21}^{AB}(\mathbf{z}) &= \mathbf{d}_1^A \cdot \mathbf{p}_1^B (M_{AB}^1)^{-1}, & \pi_{22}^{AB}(\mathbf{z}) &= \mathbf{d}_1^A \cdot \mathbf{p}_2^B (M_{AB}^2)^{-1}, & \pi_{23}^{AB}(\mathbf{z}) &= \mathbf{d}_2^A \cdot \mathbf{p}_\varphi^B, \\ \pi_{25}^{AB}(\mathbf{z}) &= \mathbf{d}_2^A \cdot \mathbf{p}_2^B (M_{AB}^2)^{-1}, & \pi_{26}^{AB}(\mathbf{z}) &= \mathbf{d}_3^A \cdot \mathbf{p}_\varphi^B, & \pi_{27}^{AB}(\mathbf{z}) &= \mathbf{d}_3^A \cdot \mathbf{p}_1^B (M_{AB}^1)^{-1}, \\ \pi_{28}^{AB}(\mathbf{z}) &= \mathbf{d}_3^A \cdot \mathbf{p}_2^B (M_{AB}^2)^{-1}, & \pi_{24}^{AB}(\mathbf{z}) &= \mathbf{d}_1^A \cdot \mathbf{p}_2^B (M_{AB}^2)^{-1} + \mathbf{d}_2^A \cdot \mathbf{p}_1^B (M_{AB}^1)^{-1}, \end{aligned} \tag{31}$$

$A, B = 1, \dots, n_{\text{node}}$. According to Theorem 2.17 in [14] (cf. Remark 8) one can choose $d = 21n_{\text{node}} - 3$ functionally independent invariants of those given in (31), generating the maximal set $\mathbf{\Pi}$, in which the Hamiltonian can be parametrised.

3.4.2. Temporal discretisation—discrete derivative

The proofs of Propositions 3.2 and 3.5 in [1] hold for a class of energy-conserving time-stepping schemes that have been derived using the discrete derivative D defined by Gonzalez [7]. The definition relies on the properties (i) directionality and (ii) consistency and leads to an energy-conserving one-step scheme. In order to transfer also the conservation of a momentum map along the solution of a Hamiltonian system to the discrete system, a G -equivariant discrete derivative D^G must be used, which fulfills the properties (iii) equivariance and (iv) orthogonality additionally to (i) and (ii). The following example of a G -equivariant discrete derivative is given in [7], where also a proper definition can be found.

Example 9. Let $\mathbf{x}, \mathbf{y} \in \mathcal{P}$, $\mathbf{w} = \frac{1}{2}[\mathbf{x} + \mathbf{y}]$ and $f : \mathcal{P} \rightarrow \mathbb{R}$ be a smooth G -invariant function with the associated reduced function $\widehat{f}(\mathbf{\Pi}(\mathcal{P})) \rightarrow \mathbb{R}$, i.e. $\widehat{f}(\mathbf{\Pi}(\mathbf{x})) = f(\mathbf{x}) \forall \mathbf{x} \in \mathcal{P}$. If the invariants π_1, \dots, π_d are at most quadratic, then a G -equivariant discrete derivative for f is given by

$$D^G f(\mathbf{x}, \mathbf{y}) = D\widehat{f}(\mathbf{\Pi}(\mathbf{x}), \mathbf{\Pi}(\mathbf{y})) \circ D\mathbf{\Pi}(\mathbf{w}) = D^T \mathbf{\Pi}(\mathbf{w}) \cdot D\widehat{f}(\mathbf{\Pi}(\mathbf{x}), \mathbf{\Pi}(\mathbf{y})). \tag{32}$$

For the discrete derivative D for example the following second-order approximation to the exact derivative at the midpoint can be used:

$$Df(\mathbf{x}, \mathbf{y}) = Df(\mathbf{w}) + \frac{f(\mathbf{y}) - f(\mathbf{x}) - Df(\mathbf{w})[\mathbf{y} - \mathbf{x}]}{\|\mathbf{y} - \mathbf{x}\|^2} [\mathbf{y} - \mathbf{x}]. \tag{33}$$

A discrete approximation of Hamilton's differential equations (1) is given by

$$\mathbf{z}_{n+1} - \mathbf{z}_n = h\mathbf{X}_H(\mathbf{z}_n, \mathbf{z}_{n+1}) = h\mathbb{J} \cdot \mathbf{D}^G H(\mathbf{z}_n, \mathbf{z}_{n+1}), \quad (34)$$

where $h > 0$ is the time step and $\mathbf{X}_H : \mathcal{P} \rightarrow T\mathcal{P}$ is the discrete Hamiltonian vector field, defined in terms of the G -equivariant discrete derivative of the Hamiltonian $\mathbf{D}^G H$. It is proven in [7] that a solution of (34) is energy–momentum conserving. This concept constitutes a special method within the family of time-stepping schemes emanating from finite element approximations in time. The crucial advantage is, that the formulas (32) and (33) are given in closed form. Thus the conservation properties do not depend on the numerical solution of arising time integrals. In [15] the motion of a constrained four particle system is calculated using the concept of the G -equivariant discrete derivatives.

3.4.3. Fully-discrete Hamiltonian system for the beam in terms of invariants

According to the spatial finite element discretisation (14), the phase space variable (15) at time t_n is given by

$$\mathbf{z}_n^h(s) = \mathbf{z}^h(s, t_n) = \sum_{A=1}^{n_{\text{node}}} N_A(s) \mathbf{z}_n^A \in \mathbb{R}^{21}, \quad n \in \mathbb{N}, \quad (35)$$

with $\mathbf{z}_n^A = \mathbf{z}^A(t_n)$, $A = 1, \dots, n_{\text{node}}$.

Definition 10. Let the pair of indices AB , where $A, B = 1, \dots, n_{\text{node}}$ be symbolised by the single index $C = 1, \dots, n_{\text{node}}^2$.

Using (16), (31) and $t_1 = 5$, $t_2 = 6$, $t_3 = 7$, the kinetic energy at time t_n can be written in the form

$$\widehat{T}^h(\mathbf{\Pi}(\mathbf{z}_n)) = \sum_{i=1}^3 \sum_{C=1}^{n_{\text{node}}^2} \widehat{T}_i^h(\pi_{\nu_i}^C(\mathbf{z}_n)) = \frac{1}{2} \sum_{C=1}^{n_{\text{node}}^2} (M_C)^{-1} \pi_5^C(\mathbf{z}_n) + (M_C^1)^{-1} \pi_6^C(\mathbf{z}_n) + (M_C^2)^{-1} \pi_7^C(\mathbf{z}_n), \quad (36)$$

where M_C , M_C^1 , M_C^2 are the entries of the consistent mass matrix (17), see Remark 4.

Inspection of the constraints (11) obviously shows on which invariants in (31) the constraints at the node A do depend on. With $p_1 = 2$, $p_2 = 3$, $p_3 = 4$, $p_4 = 11$, $p_5 = 12$, $p_6 = 13$ the function to treat the constraints (18) at time t_n can be written as

$$\widehat{P}^h(\mathbf{\Pi}(\mathbf{z}_n)) = \sum_{A=1}^{n_{\text{node}}} \mathbf{v}^A(t_n) \mathbf{R}(\widehat{g}_1(\pi_{p_1}^{AA}(\mathbf{z}_n)), \dots, \widehat{g}_6(\pi_{p_6}^{AA}(\mathbf{z}_n))). \quad (37)$$

With $\Gamma_1 = 8$, $\Gamma_2 = 9$, $\Gamma_3 = 10$, $k_1 = 13$, $k_2 = 12$, $k_3 = 11$ the objective strain measures $\mathbf{\Gamma}(\mathbf{q}^h)$, $\mathbf{K}(\mathbf{q}^h)$ at time t_n take the form

$$\begin{aligned} \widehat{\Gamma}_i(\mathbf{\Pi}(\mathbf{z}_n^h)) &= \sum_{A,B=1}^{n_{\text{node}}} N_A(s) N'_B(s) \pi_{\Gamma_i}^{AB}(\mathbf{z}_n) - \delta_{i3}, \quad i = 1, 2, 3, \\ \widehat{K}_i(\mathbf{\Pi}(\mathbf{z}_n^h)) &= \sum_{A,B=1}^{n_{\text{node}}} N_A(s) N'_B(s) [\pi_{k_i}^{AB}(\mathbf{z}_n) - \pi_{k_i}^{AB}(\mathbf{z}_0)], \quad i = 1, 2, 3. \end{aligned} \quad (38)$$

Assuming that also the external energy density function is invariant under the action of $SO(3)$ (cf. Remark 20), thus $W_{\text{ext}}(\mathbf{z}_n^h) = \widehat{W}_{\text{ext}}(\mathbf{\Pi}(\mathbf{z}_n^h))$, the potential energy (19) at time t_n reads

$$\widehat{V}^h(\mathbf{\Pi}(\mathbf{z}_n)) = \int_0^L W_{\text{int}}(\widehat{\mathbf{\Gamma}}(\mathbf{\Pi}(\mathbf{z}_n^h)), \widehat{\mathbf{K}}(\mathbf{\Pi}(\mathbf{z}_n^h))) \, ds + \int_0^L \widehat{W}_{\text{ext}}(\mathbf{\Pi}(\mathbf{z}_n^h)) \, ds. \quad (39)$$

Of course the integrals transform to sums over the nodes due to the spatial discretisation (35).

Summarising, the $SO(3)$ -invariant Hamiltonian of the beam at time t_n is of the form

$$H^h(\mathbf{z}_n) = \widehat{H}^h(\boldsymbol{\Pi}(\mathbf{z}_n)) = \widehat{T}^h(\boldsymbol{\Pi}(\mathbf{z}_n)) + \widehat{V}^h(\boldsymbol{\Pi}(\mathbf{z}_n)) + \widehat{P}^h(\boldsymbol{\Pi}(\mathbf{z}_n)). \tag{40}$$

Using (40) to set up the G -equivariant discrete derivative of the Hamiltonian in (34), one arrives at the fully-discrete constrained Hamiltonian equations for the dynamics of the geometrically exact beam, which have to be solved for $\mathbf{z}_{n+1}^A = [\mathbf{q}_{n+1}^A, \bar{\mathbf{p}}_{n+1}^A]$, $A = 1, \dots, n_{\text{node}}$

$$\begin{aligned} \bar{\mathbf{q}}_{n+1}^A - \bar{\mathbf{q}}_n^A &= h D_{\bar{\mathbf{p}}^A}^G T^h(\mathbf{z}_n, \mathbf{z}_{n+1}), \\ \bar{\mathbf{p}}_{n+1}^A - \bar{\mathbf{p}}_n^A &= -h \left[D_{\bar{\mathbf{q}}^A}^G V^h(\mathbf{z}_n, \mathbf{z}_{n+1}) + D_{\bar{\mathbf{q}}^A}^G P^h(\mathbf{z}_n, \mathbf{z}_{n+1}) \right], \\ \mathbf{0} &= -h \left[D_{\mathbf{d}_3^A}^G V^h(\mathbf{z}_n, \mathbf{z}_{n+1}) + D_{\mathbf{d}_3^A}^G P^h(\mathbf{z}_n, \mathbf{z}_{n+1}) \right]. \end{aligned} \tag{41}$$

3.5. Overview

The following table gives an overview over the phase vector, the Hamiltonian and the Hamiltonian equations corresponding to the continuous, the semi-discrete and the fully discrete case respectively.

	Phase vector	Hamiltonian	H. e.
Continuous	$\mathbf{z}(s, t) = [\mathbf{q}(s, t), \bar{\mathbf{p}}(s, t)] \in \mathbb{R}^{21}$ (6)	$H(\mathbf{z}) = T(\mathbf{z}) + V(\mathbf{z}) + P(\mathbf{z})$ (4)	(13)
Semi-discrete	$\mathbf{z}^h(s, t) = \sum_{A=1}^{n_{\text{node}}} N_A(s) \mathbf{z}^A(t) \in \mathbb{R}^{21}$ (14) $\mathbf{z}^A(t) = [\mathbf{q}^A(t), \bar{\mathbf{p}}^A(t)] \in \mathbb{R}^{21}, A = 1, \dots, n_{\text{node}}$ $\mathbf{z}(t) = [\mathbf{z}^1(t), \dots, \mathbf{z}^{n_{\text{node}}}(t)] \in \mathbb{R}^{21n_{\text{node}}}$	$H(\mathbf{z}^h) = H^h(\mathbf{z}) =$ $T^h(\mathbf{z}) + V^h(\mathbf{z}) + P^h(\mathbf{z})$ (16) (19) (18)	(25)
Fully discrete	$\mathbf{z}_n^h(s) = \sum_{A=1}^{n_{\text{node}}} N_A(s) \mathbf{z}_n^A \in \mathbb{R}^{21}, n \in \mathbb{N}$ (35) $\mathbf{z}_n^A = [\mathbf{q}_n^A, \bar{\mathbf{p}}_n^A] \in \mathbb{R}^{21}, A = 1, \dots, n_{\text{node}}$ $\mathbf{z}_n = [\mathbf{z}_n^1, \dots, \mathbf{z}_n^{n_{\text{node}}}] \in \mathbb{R}^{21n_{\text{node}}}$	$H(\mathbf{z}_n^h) = \widehat{H}^h(\boldsymbol{\Pi}(\mathbf{z}_n))$ (40)	(41)

3.6. Time-stepping scheme for the beam dynamics

In this section, we deduce the actual fully discrete Hamiltonian equations for the dynamics of the geometrically exact beam, which is a nonlinear, objective, energy–momentum-conserving one-step scheme. According to (41), we have to calculate G -equivariant discrete derivatives of T , V and P . We apply directly the formulas (32) and (33), given in Example 9 and denote the midpoint of two subsequent states of the beam by $\mathbf{z}_{n+\frac{1}{2}} = \frac{1}{2}[\mathbf{z}_{n+1} + \mathbf{z}_n]$. For the kinetic energy (36) we obtain the following:

$$D_{\bar{\mathbf{p}}^A}^G T^h(\mathbf{z}_n, \mathbf{z}_{n+1}) = \sum_{i=1}^3 \sum_{C=1}^{n_{\text{node}}^2} D \widehat{T}_i^h(\pi_{t_i}^C(\mathbf{z}_n), \pi_{t_i}^C(\mathbf{z}_{n+1})) \circ D \pi_{t_i}^C(\mathbf{z}_{n+\frac{1}{2}}). \tag{42}$$

Since $\hat{T}_i^h : \mathbb{R}_+ \rightarrow \mathbb{R}$, using (33) we have

$$D\hat{T}_i^h(\pi_{\mathbf{t}_i}^C(\mathbf{z}_n), \pi_{\mathbf{t}_i}^C(\mathbf{z}_{n+1})) = \frac{\hat{T}_i^h(\pi_{\mathbf{t}_i}^C(\mathbf{z}_{n+1})) - \hat{T}_i^h(\pi_{\mathbf{t}_i}^C(\mathbf{z}_n))}{\pi_{\mathbf{t}_i}^C(\mathbf{z}_{n+1}) - \pi_{\mathbf{t}_i}^C(\mathbf{z}_n)} =: S_{\hat{T}_i}^C, \quad i = 1, 2, 3. \quad (43)$$

From (36) we can calculate

$$S_{\hat{T}_1}^C = \frac{1}{2}M_C^{-1}, \quad S_{\hat{T}_2}^C = \frac{1}{2}(M_C^1)^{-1}, \quad S_{\hat{T}_3}^C = \frac{1}{2}(M_C^2)^{-1}. \quad (44)$$

Remark 11. For many methods to treat the constraints (e.g. Lagrange multiplier method, Penalty method, augmented Lagrange method), (37) can be transformed to $\hat{P}^h(\boldsymbol{\Pi}(\mathbf{z}_n)) = \sum_{i=1}^m \sum_{A=1}^{n_{\text{node}}} \hat{P}_i^h(\pi_{\mathbf{p}_i}^{AA}(\mathbf{z}_n))$ and the G -equivariant discrete derivative can be calculated along the lines of (42) and (43). For the three methods mentioned, the scalars $S_{\hat{P}_i}^A$, $i = 1, \dots, 6$ will be specified in the following subsections accordingly.

Because of the parametrisation of the Hamiltonian and particularly the stored energy in the quadratic invariants and the special strain measures (10) in the beam theory being in use in this work, an energy–momentum time-stepping scheme is obtained by application of the G -equivariant discrete derivative (32), (33) to the stored energy with $f = W_{\text{int}} \circ [\hat{\boldsymbol{\Gamma}}, \hat{\boldsymbol{K}}]$ and $\boldsymbol{\pi} = \boldsymbol{\Pi}$.

Remark 12. Due to the beam theory at hand and the parametrisation in the invariants, a special modification in the temporal discretisation of the stored energy terms to obtain an energy-conserving integrator (e.g. cG(1)-method in connection with the assumed strain modification in [16,17] or interpolation of the strains at different times instead of evaluation of the strains at the temporally interpolated configuration in the case of nonlinear elasticity in [18,19]) is unnecessary here.

Example 13. In the Example 6 of St. Venant-Kirchhoff material, the stored energy can be transformed into a sum of terms, each being dependent on one scalar-valued invariant $\hat{V}_{\text{int}}^h(\boldsymbol{\Pi}(\mathbf{z}_n)) = \sum_{i=1}^3 W_{\text{int}}^i(\hat{\Gamma}_i^h(\pi_{\Gamma_i}(\mathbf{z}_n)), \hat{K}_i^h(\pi_{\mathbf{k}_i}(\mathbf{z}_n)))$, thus the G -equivariant discrete derivative can be calculated along the lines of (42) and (43).

Therewith (41) can be further specified. The system of equations is implemented using the three following methods to treat the constraints. The numerical results for the example of a beam with concentrated masses are presented in Section 4.

3.6.1. Lagrange multiplier method

Using the Lagrange multiplier method, the function representing the treatment of the constraints takes the form $P_{\text{Lag}}^h(\mathbf{z}) = \boldsymbol{\lambda} \mathbf{g}(\mathbf{z})$ with the Lagrange Multiplier $\boldsymbol{\lambda} \in \mathbb{R}^m$. Here the number of constraints at each node is $m_1 = 6$ and no secondary constraints are taken into account (see Remark 2), i.e. $m = m_1$. Thus in (12) we have

$$\mathbf{v}(s, t) = \boldsymbol{\lambda}(s, t), \quad \mathbf{R}(\mathbf{g}(\mathbf{z}(s, t))) = \mathbf{g}(\mathbf{z}(s, t)) \quad (45)$$

and insertion of the interpolation (14) yields (corresponding to (18))

$$P_{\text{Lag}}^h(\mathbf{z}(t)) = \sum_{A=1}^{n_{\text{node}}} \boldsymbol{\lambda}^A(t) \mathbf{g}(\mathbf{z}^A(t)), \quad (46)$$

that can be written in terms of the invariants at time t_n as follows:

$$\hat{P}_{\text{Lag}}^h(\boldsymbol{\Pi}(\mathbf{z}_n)) = \sum_{i=1}^6 \sum_{A=1}^{n_{\text{node}}} \lambda_i^A(t_n) \hat{g}_i(\pi_{p_i}^{AA}(\mathbf{z}_n)). \tag{47}$$

In the G -equivariant discrete derivative $D^G P_{\text{Lag}}^h$, the scalars corresponding to (43) take the following values:

$$\begin{aligned} S_{\hat{P}_{\text{Lag}_i}^A}^A &= \frac{1}{2} \lambda_i^A, \quad i = 1, 2, 3, \quad A = 1, \dots, n_{\text{node}}, \\ S_{\hat{P}_{\text{Lag}_i}^A}^A &= \lambda_i^A, \quad i = 4, 5, 6, \quad A = 1, \dots, n_{\text{node}}. \end{aligned} \tag{48}$$

Remark 14. The use of Dirac deltas as shape functions for $\mathbf{v} = \boldsymbol{\lambda}$ in (14) allows the multipliers to be discontinuous across the space element boundaries. We allow discontinuity of the multipliers across time elements as well, particularly we assume the multipliers at each node to be constant during the time interval $[t_n, t_{n+1}]$ and to have a jump at the points of time t_n . For this reason all multipliers appearing in the time-stepping scheme are evaluated at the new time t_{n+1} and their time dependence is not indicated in (48).

Remark 15. If the Lagrange multiplier method is used to enforce the constraints, the time-stepping system (41) is supplemented by the constraint equations $\mathbf{g}(\mathbf{z}_{n+1}) = \mathbf{0}$ resulting in an system of DAEs. Obviously for a solution of this system of equations, the constraints are fulfilled exactly (see [1] for further details).

3.6.2. Penalty method

The penalty potential being in use here is composed by a spatially and temporally constant penalty parameter $\mu \in \mathbb{R}$ and the squared norm of the constraints

$$\mathbf{v}(s, t) = \mu, \quad \mathbf{R}(\mathbf{g}(\mathbf{z}(s, t))) = \|\mathbf{g}(\mathbf{z}(s, t))\|^2. \tag{49}$$

The same steps as in the previous paragraph for the Lagrange multiplier method lead to

$$P_{\text{Pen}}^h(\mathbf{z}(t)) = \sum_{A=1}^{n_{\text{node}}} \mu \|\mathbf{g}(\mathbf{z}^A(t))\|^2 \tag{50}$$

and finally to

$$\hat{P}_{\text{Pen}}^h(\boldsymbol{\Pi}(\mathbf{z}_n)) = \sum_{i=1}^6 \sum_{A=1}^{n_{\text{node}}} \mu \hat{g}_i^2(\pi_{p_i}^{AA}(\mathbf{z}_n)). \tag{51}$$

The scalars (corresponding to (43)) arising in $D^G P_{\text{Pen}}^h$ result in

$$\begin{aligned} S_{\hat{P}_{\text{Pen}_i}^A}^A &= \frac{\mu}{4} \left[\pi_{p_i}^{AA}(\mathbf{z}_{n+1}) + \pi_{p_i}^{AA}(\mathbf{z}_n) - 2 \right], \quad i = 1, 2, 3, \quad A = 1, \dots, n_{\text{node}}, \\ S_{\hat{P}_{\text{Pen}_i}^A}^A &= \mu \left[\pi_{p_i}^{AA}(\mathbf{z}_{n+1}) + \pi_{p_i}^{AA}(\mathbf{z}_n) \right], \quad i = 4, 5, 6, \quad A = 1, \dots, n_{\text{node}}. \end{aligned} \tag{52}$$

Remark 16. For solutions of (41) using the Penalty method with increasing penalty parameters, the constraint fulfilment improves and in the limit for $\mu \rightarrow \infty$ the solutions converge to that of the corresponding Lagrange Multiplier system, which fulfils the constraints exactly (see [1] for the proof and further details).

3.6.3. Augmented Lagrange method

In the augmented Lagrange method the function to treat the constraints is the sum of those just described

$$\mathbf{v}(s, t) = \begin{bmatrix} \boldsymbol{\lambda}^k(s, t) \\ \mu \end{bmatrix}, \quad \mathbf{R}(\mathbf{g}(\mathbf{z}^k(s, t))) = \begin{bmatrix} \mathbf{g}(\mathbf{z}^k(s, t)) \\ \|\mathbf{g}(\mathbf{z}^k(s, t))\|^2 \end{bmatrix}. \quad (53)$$

Therewith it ensues

$$P_{\text{Aug}}^h(\mathbf{z}^k(t)) = \sum_{A=1}^{n_{\text{node}}} \boldsymbol{\lambda}^{A,k}(t) \mathbf{g}(\mathbf{z}^{A,k}(t)) + \mu \|\mathbf{g}(\mathbf{z}^{A,k}(t))\|^2 \quad (54)$$

and finally

$$\hat{P}_{\text{Aug}}^h(\boldsymbol{\Pi}(\mathbf{z}^k)) = \sum_{i=1}^6 \sum_{A=1}^{n_{\text{node}}} \lambda_i^{A,k}(t_n) \hat{g}_i(\pi_{p_i}^{AA}(\mathbf{z}_n^k)) + \mu \hat{g}_i^2(\pi_{p_i}^{AA}(\mathbf{z}_n^k)), \quad (55)$$

$$\boldsymbol{\lambda}^{A,0}(t_0) = \mathbf{0} \in \mathbb{R}^9, \quad \boldsymbol{\lambda}^{A,0}(t_n) = \boldsymbol{\lambda}^{A,k_{\text{max}}}(t_{n-1}),$$

$$\boldsymbol{\lambda}^{A,k+1}(t_n) = \boldsymbol{\lambda}^{A,k}(t_n) + \mu \hat{\mathbf{g}}(\pi_{p_1}^{AA}(\mathbf{z}_n^k), \dots, \pi_{p_6}^{AA}(\mathbf{z}_n^k)), \quad A = 1, \dots, n_{\text{node}}.$$

Accordingly the scalars corresponding to (43) in $D^G P_{\text{Aug}}^h$ are composed by

$$\begin{aligned} S_{\hat{P}_{\text{Aug}_i}}^{A,k} &= \frac{1}{2} \lambda_i^{A,k} + \frac{\mu}{4} \left[\pi_{p_i}^{AA}(\mathbf{z}_{n+1}^k) + \pi_{p_i}^{AA}(\mathbf{z}_n) - 2 \right], \quad i = 1, 2, 3, \quad A = 1, \dots, n_{\text{node}}, \\ S_{\hat{P}_{\text{Aug}_i}}^{A,k} &= \lambda_i^{A,k} + \mu \left[\pi_{p_i}^{AA}(\mathbf{z}_{n+1}^k) + \pi_{p_i}^{AA}(\mathbf{z}_n) \right], \quad i = 4, 5, 6, \quad A = 1, \dots, n_{\text{node}}. \end{aligned} \quad (56)$$

Remark 17. The difference between the augmented Lagrange method and the previously described methods is that first of all the multipliers are not determined as variables when the system of equations is solved, but (41) with a fixed value $\boldsymbol{\lambda}^k$ is solved for \mathbf{z}_{n+1}^k . Secondly the improvement in the constraint fulfilment is achieved by iteration: the multipliers are updated according to (55)₃ and the corresponding solution \mathbf{z}_{n+1}^{k+1} of (41) fulfils the constraints better than \mathbf{z}_{n+1}^k . In the limit for an infinite number of iterations ($k \rightarrow \infty$) the sequence of solutions converges to the solution of the corresponding Lagrange Multiplier system, which fulfils the constraints exactly and the sequence of multipliers converges to the true Lagrange Multiplier (see [1] for the proof and further details).

4. Numerical example: beam with concentrated masses

The following example represents a three-dimensional extension of the plane version previously dealt with in [20,6]. A verification of the good simulation suitability of the present formulation could be achieved by recalculation of the results documented in these works. However a three-dimensional loading is chosen here to demonstrate the performance of the present formulation in general.

The initial configuration of a beam with concentrated masses can be seen in Fig. 2. For this problem the following parameters have been used: half-length $L = 1$ m, concentrated masses $M = 10$ kg and $m = 1$ kg, mass density per reference length $A_\rho = 0.27$ kg/m, mass moment of inertia of the cross-section $M_\rho = 9 \times 10^{-8}$ kg/m, beam stiffness parameters $EI = 0.16$ Nm², $EA = 4.8 \times 10^5$ N, $GJ = 0.1230769$ Nm² and $GA = 1.84615 \times 10^5$ N. The temporally bounded external loading has the form

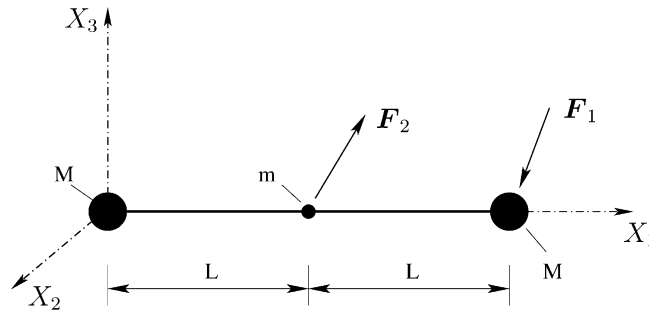


Fig. 2. Beam with concentrated masses: initial configuration.

$$\begin{aligned}
 \mathbf{F}_x = f(t)\mathbf{P}_x \quad \mathbf{P}_1 &= 1.3N\mathbf{e}_1 + 1.0N\mathbf{e}_2 + 0.8N\mathbf{e}_3, \\
 \mathbf{P}_2 &= -1.2N\mathbf{e}_1 - 1.6N\mathbf{e}_2 + 1.0N\mathbf{e}_3,
 \end{aligned}
 \tag{57}$$

with the function

$$f(t) = \begin{cases} [1 - \cos(2\pi/T)]/2 & \text{für } t \leq T, \\ 0 & \text{für } t > T \end{cases}
 \tag{58}$$

and $T = 0.5$ s.

No other external loads are present in this example. The numerical results are based on a constant time step $h = 0.01$ s and an equidistant spatial discretisation of the central line of the beam by 22 linear beam elements. The discretised configurations of the beam (calculated using the Lagrange multiplier method) at $t = 0$ s, $t = 2$ s, $t = 15$ s can be seen in Fig. 5.

4.1. Lagrange multiplier method

Using the Lagrange multiplier method the Hamiltonian equations (41) supplemented by the constraint equations $\mathbf{g}(\mathbf{z}_{n+1}) = \mathbf{0}$ are solved. The conservation properties of the algorithm can be checked in Fig. 3, after the vanishing of the external loads at $t = 0.5$ s, the total energy and the angular momentum are constant. The evolution of the conjugate stress resultants $\mathbf{n} = \frac{\partial W}{\partial \mathbf{T}}$, $\mathbf{m} = \frac{\partial W}{\partial \mathbf{K}}$ at $X_1 = L/2$ is depicted in Fig. 4. Of course using the Lagrange multiplier method the constraints are fulfilled numerically exactly, the error is of the order 10^{-16} . Although being unaccounted for, the constraints on momentum level are fulfilled up to the order 10^{-4} .

The evolution of the energy, the angular momentum and the stress resultants can be compared qualitatively to those of the two-dimensional example in [20,6].

4.2. Penalty method

The deformation of the beam with identical initial configuration and loading is calculated using the Penalty method with penalty parameter $\mu = 10^7$. The evolution of the energy and angular momentum as well as of the conjugate stress resultants at $X_1 = L/2$ can not be distinguished optically from those in Figs. 3 and 4. The error of the fulfilment of the constraints on configuration level is of the order 10^{-8} and on momentum level of the order 10^{-5} (although the secondary constraints are not enforced in the calculation) as pictured in Fig. 6 exemplarily for node 2 (second node from the left). Also for this node, the linear decrease of the configuration constraint error for increasing penalty parameters can be seen in Fig. 7. This verifies the first

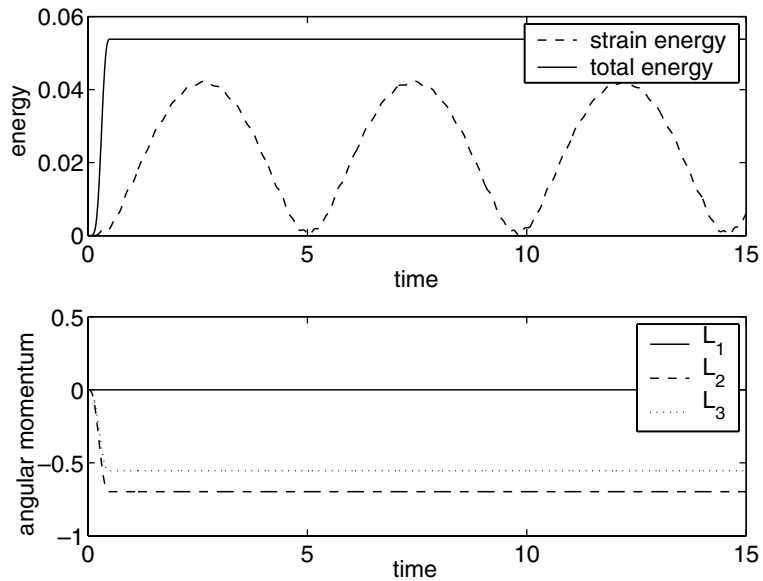


Fig. 3. Algorithmic conservation of total energy and angular momentum for $t > T$.

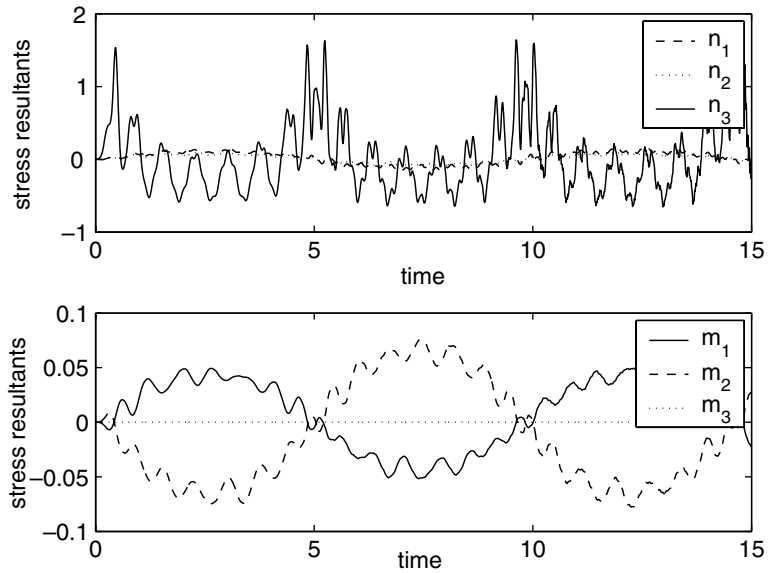


Fig. 4. Evolution of stress resultants at $X_1 = L/2$.

statement in Remark 16. The second statement, that the solution of (41) using the Penalty method converges to that of (41) using the Lagrange multiplier method is visualised in Fig. 8 for the displacements of node 12 (middle node) and of node 23 (node on the right of the beam).

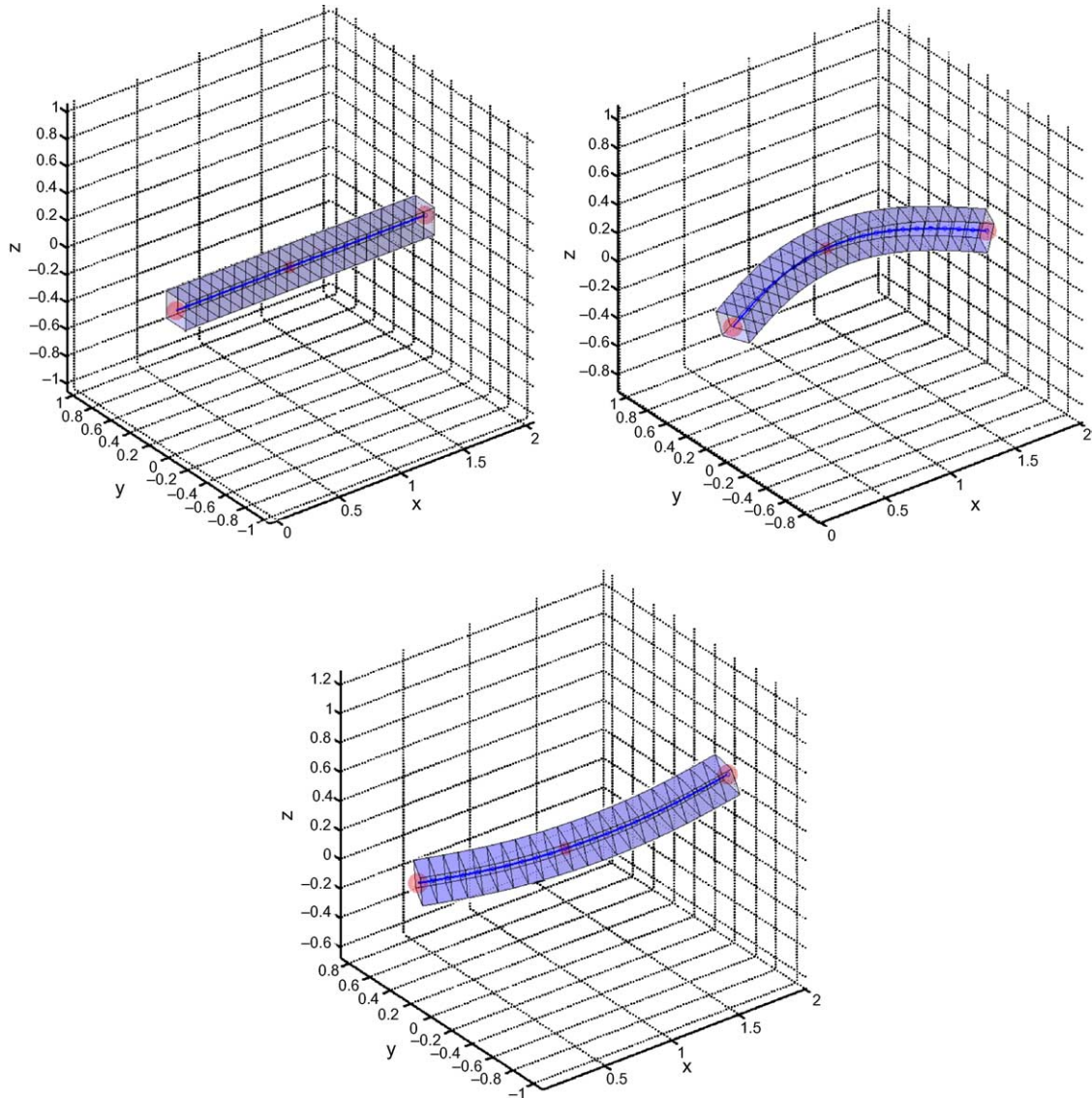


Fig. 5. Beam with concentrated masses: discrete configuration at $t = 0$ s, $t = 2$ s, $t = 15$ s.

4.3. Augmented Lagrange method

The same beam deformation problem is calculated using the augmented Lagrange method with $\mu = 10^4$. Again the evolution of the energy and angular momentum as well as of the conjugate stress resultants at $X_1 = L/2$ can not be distinguished optically from those in Figs. 3 and 4. The error of the fulfilment of the constraints at each time step at node 2 (second node from the left) on configuration level is of the order 10^{-7} and on momentum level of the order 10^{-4} (although the secondary constraints are not enforced in the calculation). All statements in Remark 17 are verified by the next three diagrams. Fig. 9 demonstrates the decrease in the error of the constraints at node 2 (second node from the left), within 4 Augmented Lagrange

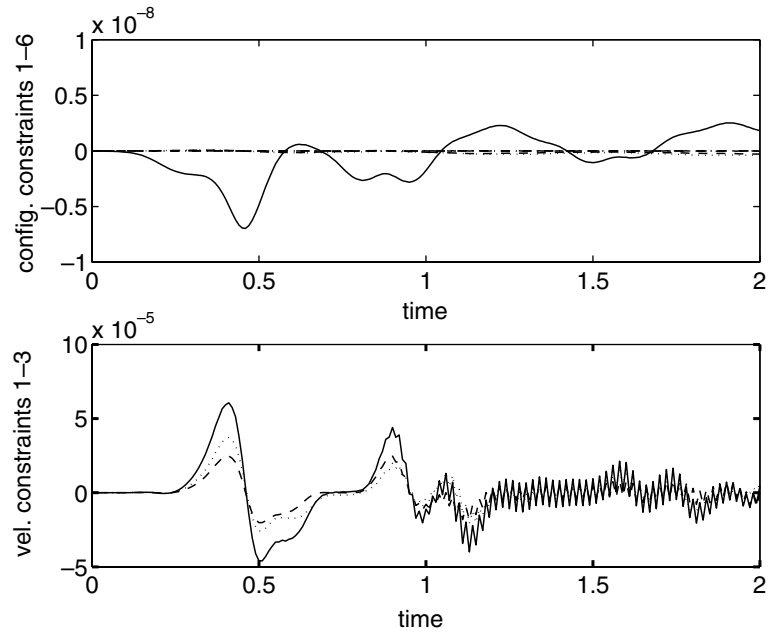


Fig. 6. Algorithmic fulfilment of the constraints at node 2, $\mu = 10^7$.

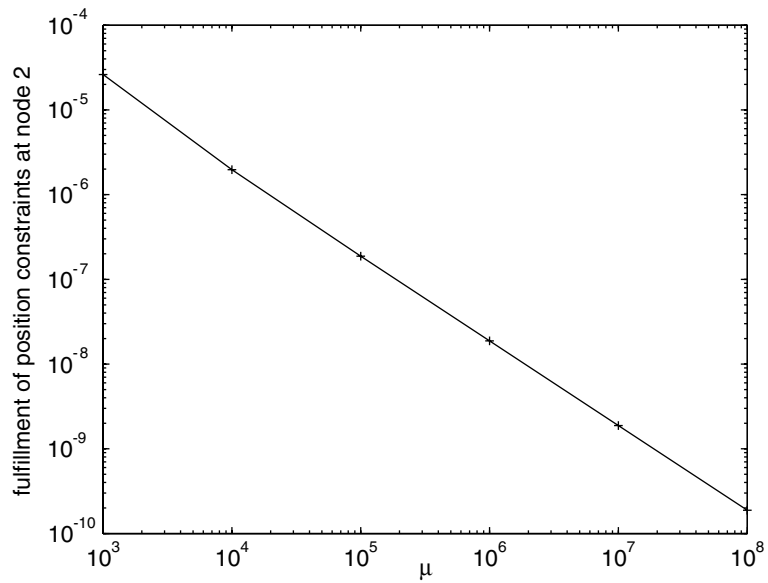


Fig. 7. Improvement of the constraint fulfilment at node 2 for increasing penalty parameters, vertical axes: $\|g(z^2)\|$.

iterations the error drops under the desired tolerance of 10^{-7} (of course, the constraint errors at all nodes are considered in the convergence criterion for the Augmented Lagrange iteration within one time step).

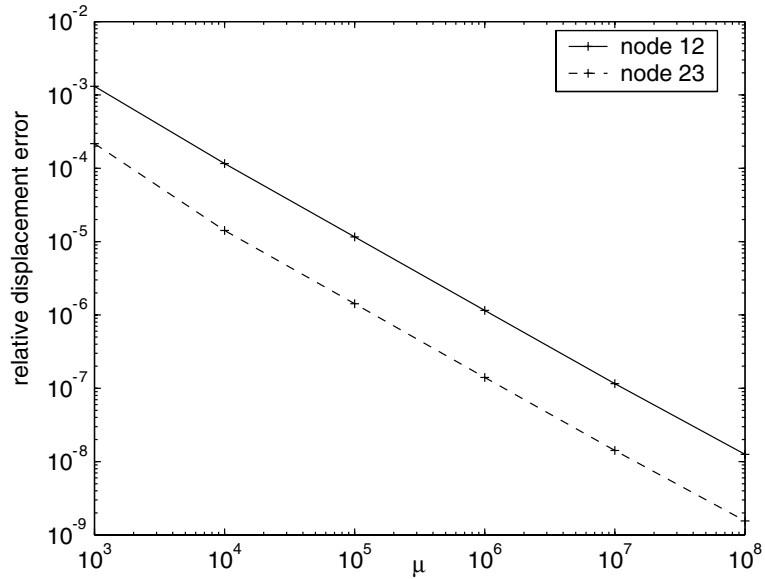


Fig. 8. Convergence of the displacements of node 12 and node 23 calculated using the Penalty method to the displacements calculated using the Lagrange multiplier method for increasing penalty parameters, vertical axes: $\frac{\|\varphi_{pen}^A - \varphi_{Lag}^A\|}{\|\varphi_{Lag}^A\|}$, $A = 12, 23$.

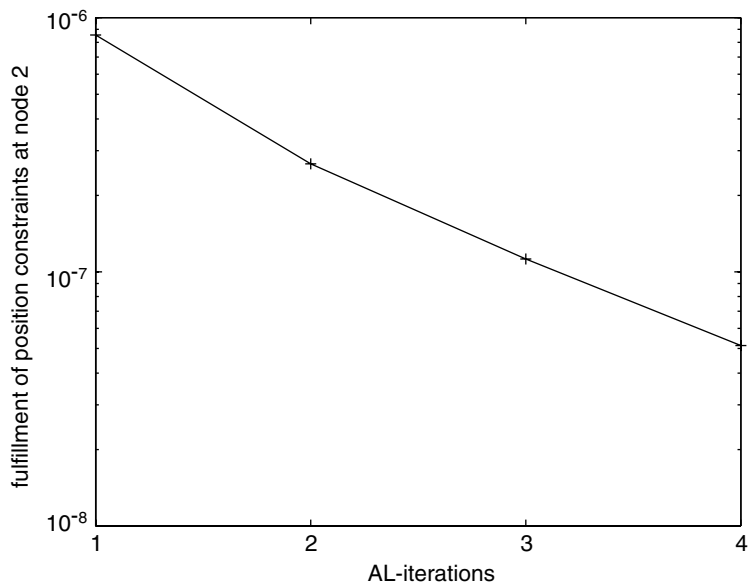


Fig. 9. Improvement of the constraint fulfilment at node 2 during AL-iteration, $\mu = 10^4$, vertical axes: $\|g(z^2)\|$.

The convergence of the displacements of node 12 (middle node) and of node 23 (node on the right of the beam) calculated by solving (41) using the augmented Lagrange method to those calculated by solving (41) using the Lagrange multiplier method is depicted in Fig. 10. Similarly the multipliers at node 2 (second

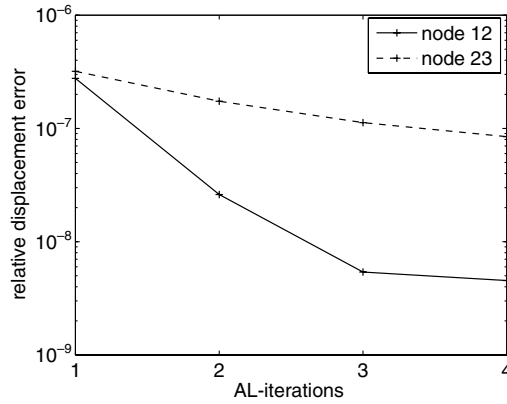


Fig. 10. Convergence of the displacements of node 12 and node 23 calculated using the augmented Lagrange method to the displacements calculated using the Lagrange multiplier method during AL-iteration, $\mu = 10^4$, vertical axes: $\frac{\|\phi_{Aug}^A - \phi_{Lag}^A\|}{\|\phi_{Lag}^A\|}$, $A = 12, 23$.

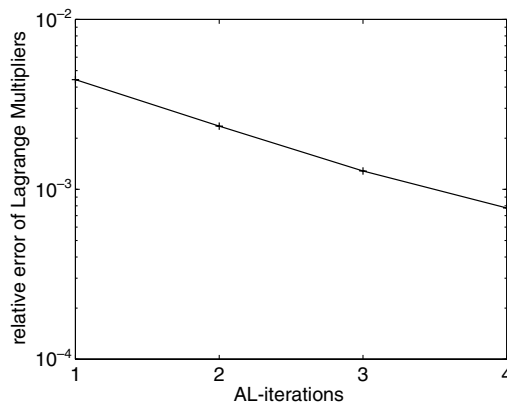


Fig. 11. Convergence of the multipliers of node 2 calculated using the augmented Lagrange method to the true Lagrange Multipliers during AL-iteration, $\mu = 10^4$, vertical axes: $\frac{\|\lambda_{Aug}^2 - \lambda_{Lag}^2\|}{\|\lambda_{Lag}^2\|}$.

node from the left) approach the true Lagrange Multipliers during the Augmented Lagrange iteration, as can be seen in Fig. 11.

5. Conclusions

The formulation of semi-discrete equations of motion for geometrically nonlinear beam dynamics as constrained Hamiltonian system states an unified framework for the use of different methods for the constraint enforcement and for the consideration of different types of constraints. Internal constraints, which are associated with the kinematic assumptions of the underlying continuous formulation, as well as external constraints, realising joints between (rigid or flexible) components of multibody systems, can be dealt with in a similar, systematic way.

Since the director triad at each point of the central line of the beam represents the configuration variable, and the semi-discrete strain measures do depend on scalar products of those vectors, these strain measures are objective. Furthermore assuming that the total Hamiltonian is invariant with respect to proper rotations, it can be parametrised in the invariants of the Lie group $SO(3)$, what states an ideal basis for a temporal discretisation using the concept of G -equivariant discrete derivatives by Gonzalez [7]. Altogether this leads to objective energy–momentum conserving time-integration of the equations of motion.

The propositions about the equivalence of the discrete Penalty system (in the limit for increasing penalty parameters) and of the discrete Augmented Lagrange system (in the limit for infinitely many iterations) to the discrete Lagrange Multiplier system proved in [1] could be illustrated for spatially discretised problems at the example of a beam with concentrated masses. Thereby it is interesting to note, that the secondary constraints on momentum level were fulfilled equally well for the different methods to treat the constraints, although only the configuration constraints have been enforced in the equations of motion.

References

- [1] S. Leyendecker, P. Betsch, P. Steinmann, Energy-conserving integration of constrained Hamiltonian systems—a comparison of approaches, *Comput. Mech.* 33 (2004) 174–185.
- [2] S. Antmann, *Nonlinear Problems in Elasticity*, Springer, Berlin, 1995.
- [3] J. Simo, A finite strain beam formulation. The three-dimensional dynamic problem. Part I, *Comput. Methods Appl. Mech. Engrg.* 49 (1985) 55–70.
- [4] I. Romero, F. Armero, An objective finite element approximation of the kinematics of geometrically exact rods and its use in the formulation of an energy–momentum scheme in dynamics, *Int. J. Numer. Methods Engrg.* 54 (2002) 1683–1716.
- [5] P. Betsch, P. Steinmann, Frame-indifferent beam finite elements based upon the geometrically exact beam theory, *Int. J. Numer. Methods Engrg.* 54 (2002) 1775–1788.
- [6] P. Betsch, P. Steinmann, Constrained dynamics of geometrically exact beams, *Comput. Mech.* 31 (2003) 49–59.
- [7] O. Gonzalez, Time integration and discrete Hamiltonian systems, *J. Non-linear Sci.* 6 (1996) 449–467.
- [8] J. Wendlandt, J. Marsden, Mechanical integrators derived from a discrete variational principle, *Physica D* 106 (1997) 223–246.
- [9] D. Luenberger, *Introduction to Linear and Nonlinear Programming*, Addison-Wesley, Reading, MA, 1973.
- [10] H. Rubin, P. Ungar, Motion under a strong constraining force, *Commun. Pure Appl. Math.* 10 (1) (1957) 65–87.
- [11] D. Bertsekas, *Nonlinear Programming*, Athena Scientific, Belmont, Massachusetts, 1995.
- [12] P. Dirac, On generalized Hamiltonian dynamics, *Can. J. Meth.* 2 (1950) 129–148.
- [13] W. Seiler, Numerical integration of constrained Hamiltonian systems using Dirac brackets, *Math. Comput.* 68 (226) (1999) 661–681.
- [14] P. Olver, *Applications of Lie Groups to Differential Equations*, Graduate Texts in Mathematics, Springer, Berlin, 1986.
- [15] O. Gonzalez, Mechanical systems subject to holonomic constraints: differential-algebraic formulations and conservative integration, *Physica D* 132 (1999) 165–174.
- [16] P. Betsch, P. Steinmann, Conserving properties of a time FE method—Part II: Time-stepping schemes for non-linear elastodynamics, *Int. J. Numer. Methods Engrg.* 50 (2001) 1931–1955.
- [17] J. Simo, T. Hughes, On the variational foundations of assumed strain methods, *J. Appl. Mech.* 53 (1986) 51–54.
- [18] J. Simo, N. Tarnow, The discrete energy–momentum method. Conserving algorithms for nonlinear elastodynamics, *ZAMP* 43.
- [19] O. Gonzalez, Exact energy–momentum conserving algorithms for general models in nonlinear elasticity, *Comput. Methods Appl. Mech. Engrg.* 190 (2000) 1763–1783.
- [20] C. Bottasso, O. Bauchau, J. Choi, An energy decaying scheme for nonlinear dynamics of shells, *Comput. Methods Appl. Mech. Engrg.* 191 (2002) 3099–3121.